Lattice simulation of the BFSS model

Project under the DAAD-WISE program

Report by
Adithya A Rao
National Institute of Technology, Surat

Supervisor
Dr. habil. Georg Bergner
Theoretisch-Physikalische Institut
Friedrich-Schiller-Universität Jena

Summer 2023

Acknowledgement

I would like to express my sincere gratitude to Dr. habil. Georg Bergner for agreeing to supervise this project and his invaluable guidance and supervision throughout this project. His expertise and insights have been instrumental in shaping this research work. I also thank Ivan Soler Calero for putting through my questions and always answering them patiently.

I am also deeply thankful to the DAAD-WISE program for providing me with this wonderful opportunity to engage in this enriching research experience. Their support has been crucial in making this project possible and contributing to my academic growth.

ADITHYA A RAO

Contents

1 Introduction

The BFSS matrix model, named after its creators Tom Banks, Willy Fischler, Stephen Shenker, and Leonard Susskind, is a significant framework in theoretical physics that emerged in the mid-1990s. It describes the dynamics of a large number of D0-branes in string theory, particularly in the context of M-theory, which is a proposed unifying theory of all string theories. The model operates in a non-commutative geometric framework, where the Bosonic degrees of freedom are represented by a set of large matrices. These matrices encapsulate the interactions and configurations of D0-branes, allowing researchers to explore the strong coupling limit of string theory. The BFSS model has been instrumental in advancing our understanding of M-theory and has inspired various extensions and related models, including the IKKT matrix model, which further investigates the relationship between matrix theory and non-commutative geometry.

The BFSS model can be viewed as a Supersymmetric Yang-Mills theory in one-dimensional time, where the Bosonic degrees of freedom are represented by $N \times N$ Hermitian matrices. These matrices correspond to the coordinates of the D0-branes, and their dynamics are governed by an action that includes kinetic terms, interaction terms, and Fermionic contributions, all of which are essential for maintaining supersymmetry. As N becomes large, the model captures non-perturbative effects and reveals a rich structure. Furthermore, the BFSS model serves as a bridge to M-theory, suggesting that the dynamics of D0-branes can be interpreted in terms of a higher-dimensional theory.

This project aims to simulate the behavior of the BFSS model on a lattice. The C++ code for the simulation, the data analysis notebooks and a brief description of my contributions to the project, are in the Github repository https://github.com/adithyarao3103/BFSS-CPPCODE/. The repository also hosts a C++ code for lattice simulation of $SU(2)$ gauge theory, written by me to illustrate the basic lattice simulation techniques.

2 Prelude: Gauge Theories on the Lattice

Lattice formulation is the only known non-perturbative, regularized formalism for Quantum Field Theories. The path integrals in the Euclidean space-time are only defined formally. They have exact definitions only in the case of finite degrees of freedom. In the path integral, the $\mathcal{D}\phi$ implies we are performing integration over the values of the fields at each point in space-time. This is a system with infinite degrees of freedom, making the integrals ill-defined when it comes to exact prescriptions.

Thus to give the path integrals a precise meaning, there arises a need to make the degrees of freedom finite, i.e., to discretize space-time, forming a lattice. In lattice field calculation, one discretizes the space-time, forming a finite periodic lattice, on which the (finite) path integral is performed. The

actual path integrals are obtained back from the lattice calculations by taking the continuum limit, i.e. lattice spacing $a \to 0$ and also the thermodynamic limit, $N \to \infty$ where N is the number of lattice sites.

Here we discuss the lattice gauge theories in brief as a prelude to the implementation of the BFSS model on the lattice.

2.1 Discretized Calculus and the Lattice Action

The central idea of Lattice Field theory is to replace the continuum of space-time with a discretized lattice. The choice of this lattice is not unique, there exist a multitude of choices, but usually one takes the simplest possible one, the 4-dimensional hypercube, with lattice points on the corners only. This prescription means the replacement

$$\mathbf{x} \to a\mathbf{n}, \quad n_i = 0, 1, \ldots, N-1, \quad \text{for} \quad i = 1, 2, 3, 4 \tag{1}$$

where a is the lattice spacing.
This gives rise to the lattice with N^4 sites. Since having a boundary gives rise to boundary effects that do not go away when taking the thermodynamic limit, we need to specify what happens at the boundary points. Usually lattices with boundaries identified are considered, i.e., we identify the sites $n_j = N$ and $n_j = 0$ as the same. Further, the boundary conditions apply to fields too, where for Bosonic fields we take periodic boundary conditions, $\Phi(a(n+N)) = \Phi(n)$, while for Fermionic fields we consider anti-periodic boundary conditions $\Psi(a(n+N)) = -\Psi(n)$

With this discretization, the fields now live on the lattice sites, i.e.

$$\Phi(\mathbf{x}) \to \Phi(a\mathbf{n}) \tag{2}$$

Again, there are multiple versions of derivatives one can implement on a discrete lattice, the simplest examples being the central difference derivative, forward difference derivatives, etc. Different lattices and different discretized derivatives have different errors. For example, the central difference derivative has error $\mathcal{O}(a^2)$, while the forward and backward difference derivatives have $\mathcal{O}(a)$. It is possible to construct more accurate lattices and derivatives, but usually the prescribed discretization is accurate enough.

We therefore replace the derivatives in the action with

$$\partial_{\mathbf{j}}\Phi(a\mathbf{n}) = \frac{\Phi(a\mathbf{n}+\mathbf{j}) - \Phi(a\mathbf{n}-\mathbf{j})}{2a^2} + \mathcal{O}(a^2) \tag{3}$$

and the spacetime integrals are replaced by

$$\int d^4x \to a^4 \sum_{\text{all lattice sites}} \tag{4}$$

Lattice formulation of the field theory would simply mean discretizing the action on a spacetime lattice in the prescription given above and calculating the path integral, which is now reduced to a sum over all configurations by using Monte Carlo methods.

2.2 Gauge Theory on the Lattice

The local gauge invariance of the Dirac fields, but considering the fields to be on the space-time lattice rather than on the continuum.

The local gauge invariance implies that the Dirac action should not change under the transformation

$$\Psi(\mathbf{n}) \to G(\mathbf{n})\Psi(\mathbf{n}) \tag{5}$$

where the G's belong to the group $\mathcal{G}$, $G(\mathbf{n}) \in \mathcal{G}$.(we have suppressed the lattice spacing a in the equations).

As is the case in the continuum, the derivatives in the lattice case also are ill-defined without defining the parallel transporter on the lattice. The parallel transporter is necessary to make comparisons of field values at two different sites consistent under the action of a local gauge transformation. It would not make sense to compare fields at two different sites if the gauge transformation acting on the two is not the same. The parallel transporter gives an object that has the same gauge transformation as that on the said site, allowing us to consistently compare the values at the two sites.

The parallel transporter is of the same form as in the continuum case, with the transformation law being

$$U(n_i, n_j) \to G(n_i)U(n_i, n_j)G(n_j)^{-1} \tag{6}$$

With this, the consistent (Covariant) discrete derivative reads

$$D_{\mathbf{j}}\Phi(\mathbf{n}) = \frac{U(\mathbf{n}, \mathbf{n}+\mathbf{j})\Phi(\mathbf{n}+\mathbf{j}) - U(\mathbf{n}, \mathbf{n}-\mathbf{j})\Phi(\mathbf{n}-\mathbf{j})}{2a^2} + \mathcal{O}(a^2) \tag{7}$$

These parallel transporters are not present on the lattice sites, but rather live on the links between the lattice sites, and are hence called as link variables. We denote by $U_\mu(n)$ the link variable connecting the sites $U(n)$ & $U(n, n+\mu)$, where $\mu \in \{1, 2, \ldots, d\}$. This means that the link variables

are oriented, and therefore we can introduce the notation $U_{-\mu}(n) = U(n, n-\mu) \equiv U(n-\mu, n)^{-1}$.

In a lattice gauge theory, it is these link variables that play the role of the gauge fields. Unlike the continuum theory, where the gauge fields are *algebra valued*, the gauge fields in the lattice are *group valued*. This constitutes a huge difference in the two theories, since in the case of the standard model, the algebra is non-compact, on the other hand, the group is compact.

With such a construction, a 2-dimensional spacetime with 3 sites in each dimension, with periodic boundary conditions when put on a lattice, would look like

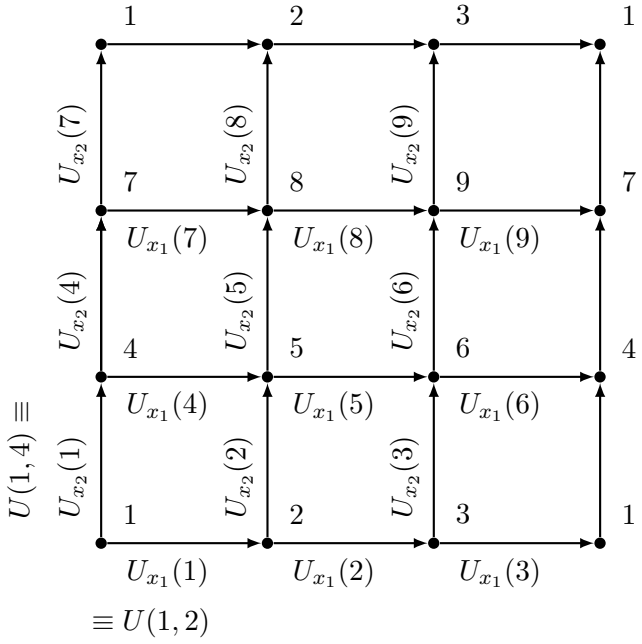

Figure 1: A 3×3 lattice discretization of a 1+1 dimensional spacetime

2.3 The Free Gauge Action

2.3.1 Gauge invariant objects from the link variables

Consider for simplicity a two-dimensional lattice. On this lattice take a chain of two links, i.e two links that share a common site, with orientation preserved while going from one to another, $U_a \equiv U_1(i-1, j)$ and $U_b \equiv U_2(i, j)$. The gauge dependency of the directional product of these two links ($U_a \times U_b$, and not $U_b \times U_a$) would not depend on the group element on the site (i, j). This is because the action of $\Omega(i, j)$ on $U_1(i-1, j)$ would be the inverse of that on $U_2(i, j)$ and hence when taking the product they would cancel each other.

Now if we consider a directional connected chain of multiple links, the gauge dependency of the

directional product would depend only on the group elements at the endpoint. If we take the chain to be a closed loop, then the gauge dependency of the oriented product of the links in the loop would depend only on the group element on the starting(ending) site. The product transforms in the adjoint representation of the group.
The trace operation maps elements in the adjoint representation of the group to a scalar which does not change under a group transformation at all, and hence the trace of the oriented product of a closed directional loop of link variables is a gauge invariant object.

That is, for a loop $L(U) = \prod_{\text{loop}} U$, the transformation would be

$$L(U) \to G(x_1)L(U)G(x_1)^{-1} \tag{8}$$

where x_1 is the starting(ending) site of the loop. Under the trace operation, due to the cyclicity of the trace, we get

$$\text{tr}L(U) \to \text{tr}(G(x_1)L(U)G(x_1)^{-1}) = \text{tr}L(U) \tag{9}$$

If U_{cl} is the set of all closed loops in the links on a lattice, then a general gauge invariant object constructed out of the links would be a function with $\{\text{tr}(u) \mid u \in U_{cl}\}$ as preimage.

2.3.2 The Wilson Gauge Action

To construct the lattice gauge action we consider the smallest possible non-trivial loop on the lattice, the plaquette variable. The plaquette variable at a site, $U_{\mu\nu}(n)$ is defined as the product of the four links,

$$\begin{aligned} U_{\mu\nu}(n) &= U_\mu(n)\ U_\nu(n+\mu)\ U_{-\mu}(n+\mu+\nu)\ U_{-\nu}(n+\nu) \\ &= U_\mu(n)\ U_\nu(n+\mu)\ U_\mu(n+\nu)^{-1}\ U_\nu(n)^{-1} \end{aligned} \tag{10}$$

The gauge action is then derived from the sum of plaquette variables at all the sites, given as

$$S \propto \sum_n \sum_{\mu<\nu} \text{Re tr } (\mathbb{I} - U_{\mu\nu}(n)) \tag{11}$$

2.4 Performing the simulation

Once we obtain the discretized theory, the next step in lattice simulations is to perform the path integrals using numerical methods. That is, we evaluate, (for a pure gauge theory),

$$\langle \mathcal{O} \rangle = \frac{1}{Z} \int \mathcal{D}U\ \mathcal{O}[U]\ \exp(-S[U]) \tag{12}$$

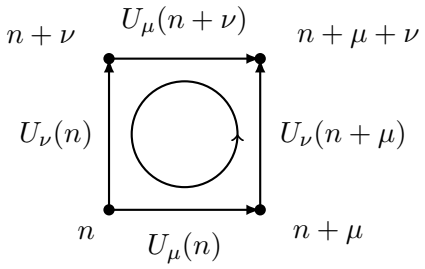

Figure 2: The plaquette variable associated with the site n

Analytical evaluation of the above integral is not possible so we use Monte-Carlo methods to perform the integration.
In naive Monte Carlo, we give the estimate to be

$$\langle \mathcal{O} \rangle \approx \langle \mathcal{O} \rangle_{MC} = \frac{1}{N} \sum_{U_n} \frac{1}{Z} \mathcal{O}[U] \exp(-S[U]) \tag{13}$$

where the U_ns are sampled uniformly randomly, with the result being exact at $N \to \infty$, i.e.,

$$\lim_{N \to \infty} \langle \mathcal{O} \rangle_{MC} = \langle \mathcal{O} \rangle$$

This method is very inefficient since the integrand is highly peaked around the classical configurations, i.e., around the minima of $S[U]$.

A better method would be to perform importance sampling, where rather than sampling the U_n randomly, we sample according to the distribution $\exp(-S[U])$, i.e. the probability of generating U being proportional to $\exp(-S[U])$. With importance sampling, the above integration reduces to

$$\langle \mathcal{O} \rangle \approx \frac{1}{N} \sum_{U_n} \mathcal{O}(U_n) \tag{14}$$

where the U_ns are sampled according to the distribution $\exp(-S[U])$.

Such a sampling can be done by using the Metropolis algorithm. The algorithm starts with a configuration U. It proposes a new configuration U' from the current configuration U, and accepts or rejects it based on the change in action $\Delta S = S[U'] - S[U]$. The new configuration is accepted with probability $\min(1, \exp(-\Delta S))$. If accepted, U' becomes the new current configuration; otherwise, U is retained. This process is repeated many times to generate a Markov chain of configurations that asymptotically samples the desired distribution. The Metropolis algorithm ensures detailed balance and ergodicity, which are crucial for correct sampling in lattice simulations.

Therefore a realisation of the Metropolis algorithm for the simulation of gauge theories can be given

as

Step 1 Given a lattice with configuration U, choose at random a site n and a direction μ and multiply the link by a random matrix $X \in \mathcal{G}$ to generate a new configuration U'.

Step 2 Obtain the change in action, $\Delta S = S[U'] - S[U]$, and subsequently $\exp(-S[U])$. Generate a random number r in the interval $[0, 1)$. If $r \leq \exp(-S[U])$, then accept U' as a new configuration. Otherwise, reject it and retain U as the new configuration. This step leads to a guaranteed acceptance if the new action is lesser than the current action. In case it is larger, there is still a possibility of acceptance. One could see this as quantum fluctuations in the configuration.

Step 3 Repeat the above steps to generate samples.

For a more comprehensive and complete discussion on Lattice Quantum Field Theory we would point the reader to the excellent textbook by Gattringer and Lang [1]

3 Simulating the BFSS Model on the Lattice

The BFSS model is obtained from the reduction of the 9+1 dimensional Supersymmetric Yang-Mills to 0+1 dimensions. It is said to be dual to type IIB string theories and arises naturally as an effective low-energy description of D0-branes.

Upon dimensional reduction, the A_μ fields of the Yang-Mills theory, which are $N \times N$ matrices of $SU(N)$, get reduced to the vector field A_t and scalar fields X_M. We can further use the gauge freedom to eliminate the vector field A_t giving an interacting quantum mechanics of 9 $N \times N$ matrices. Note that the Fermionic fields in this theory are 16 $N \times N$ matrices in the adjoint representation of $SU(N)$ and not in the fundamental representation.

The complete action of the BFSS model is therefore given by

$$S_M = \frac{1}{g^2} \int dt \, \mathrm{Tr} \left\{ \frac{1}{2}(D_0 X^M)^2 + \frac{1}{4}[X^M, X^N]^2 - \frac{i}{2}\Psi^T C_{10}\, \Gamma^0 D_0 \Psi + \frac{1}{2}\Psi^T C_{10}\, \Gamma^M [X^M, \Psi] \right\} \quad (15)$$

where

$$\begin{aligned} \Gamma^M &= \gamma^M \otimes \sigma_1 \ , \qquad \text{for } i = 1, \cdots, 9 \ , \\ \Gamma^0 &= 1_{16} \otimes i\sigma_2 \ , \\ C_{10} &= C_9 \otimes i\sigma_2 \ , \end{aligned}$$

and C_9 is the charge conjugation matrix in nine dimensions satisfying $C_9 \gamma^M C_9^{-1} = \gamma^{M^T}$ and σ_i are the Pauli matrices.

We consider this theory on a Euclidean spacetime lattice of circumference $\beta = 1/T$ with periodic boundary conditions. Here, the T is interpreted as the temperature. Therefore, at each spacetime point, there are 9 Bosonic $N \times N$ matrices X with periodic boundary conditions and 16 $N \times N$ Fermionic matrices Ψ with anti-periodic boundary conditions.

The action of the theory, when discretized, is given by

$$S = S_b + S_f \tag{16}$$

$$S_b = \frac{N}{2a} \sum_{t.M} \mathrm{Tr} \left(U X_M(t+a) U^\dagger - X_M(t) \right)^2 - \frac{Na}{4} \sum_{t.M.N} \mathrm{Tr}[X_M(t), X_N(t)]^2 \tag{17}$$

$$S_f = iN \sum_t \mathrm{Tr} \bar{\psi}(t) \begin{pmatrix} 0 & D_+ \\ D_- & 0 \end{pmatrix} \psi(t) - aN \sum_{t,M} \bar{\psi}(t) \gamma^M [X_M(t), \psi(t)] \tag{18}$$

with

$$\begin{aligned} D_+ \psi(t) &= U \psi(t+a) U^\dagger - \psi(t), \\ D_- \psi(t) &= \psi(t) - U^\dagger \psi(t-a) U \end{aligned} \tag{19}$$

The objective of the project is to simulate the dynamics of this action on the lattice. First, we wrote the Energy observable for both the purely Bosonic sector and the complete action of the BFSS model to verify the behavior of energy with respect to the temperature to ensure the code's correctness.

After verification, we studied the gauge-invariant 4-point function of the purely Bosonic BFSS model given by

$$G(\Delta t) \propto \int dt \ \langle \ \mathrm{Tr}(X_M(t) X^M(t)) \ \mathrm{Tr}(X_N(t+\Delta t) X^N(t+\Delta t)) \ \rangle \tag{20}$$

4 Numerical Techniques

We perform the simple Monte-Carlo simulation of the discussed model using the Metropolis algorithm to generate samples. We first run the Metropolis algorithm for multiple steps without performing the integration to ensure that the configuration has *thermalized*, i.e., has reached the equilibrium state. Once thermalized, we perform the integration by generating samples, obtaining the values of the observables and then averaging over the values.

Further, we employ statistical techniques to analyze the obtained data. Here we describe in brief the techniques involved in the analysis.
Suppose we have obtained the values $(O_1, O_2, \ldots, O_n)$ of the observables. The expectation value of

the observable is

$$\langle O \rangle = \frac{1}{N} \sum_{i=1}^{N} O_i \tag{21}$$

If values are uncorrelated, i.e., if $\langle O_i O_j \rangle = \langle O_i \rangle \langle O_j \rangle$ for all i, j, then the variance of the observable $\sigma_O = \langle (O - \langle O \rangle)^2 \rangle$ gives the statistical error in the observable, and one would quote the result as

$$\langle O \rangle \pm \sigma, \quad \sigma = \frac{1}{\sqrt{N}} \sigma_O \tag{22}$$

But in the case the data is correlated, we will have to employ other techniques to obtain the correct errors from the data.

In our case of the lattice simulations, since the data is a result of a computer time-series, there is a high chance that the data is not uncorrelated. I.e. the *autocorrelation function* defined as

$$C_O(O_i, O_{i+t}) = \langle \ (O_i - \langle O_i \rangle) \ (O_{i+t} - \langle O_{i+t} \rangle) \ \rangle = \langle O_i O_{i+t} \rangle - \langle O_i \rangle \langle O_{i+t} \rangle \tag{23}$$

is non-zero for the data.
We expect that the normalized autocorrelation,

$$\Gamma_O(O_i, O_{i+t}) = \frac{C_O(O_i, O_{i+t})}{\sigma_O^2} \tag{24}$$

displays approximately exponential decay.

In this case, we define the *integrated autocorrelation time* as

$$\tau_{O,\ \mathrm{int}} = \frac{1}{2} + \sum_{t=1}^{M} \Gamma_O(O_i, O_{i+t}) \tag{25}$$

where $M < N$ is the cutoff beyond which times the autocorrelator becomes unreliable, which in our case was the point at which the autocorrelator became negative.
The actual error in the observable then becomes

$$\sigma_{\langle O \rangle} = \sigma_O \sqrt{\frac{2}{N} \tau_{O,\ \mathrm{int}}} \tag{26}$$

5 Results

Here we present the results of the simulations for the gauge invariant 4-point correlators of the purely Bosonic BFSS model.

Correlators at Different Temperatures

We first simulated the correlators on a lattice of size 32, with $N = 9$ for different temperatures.

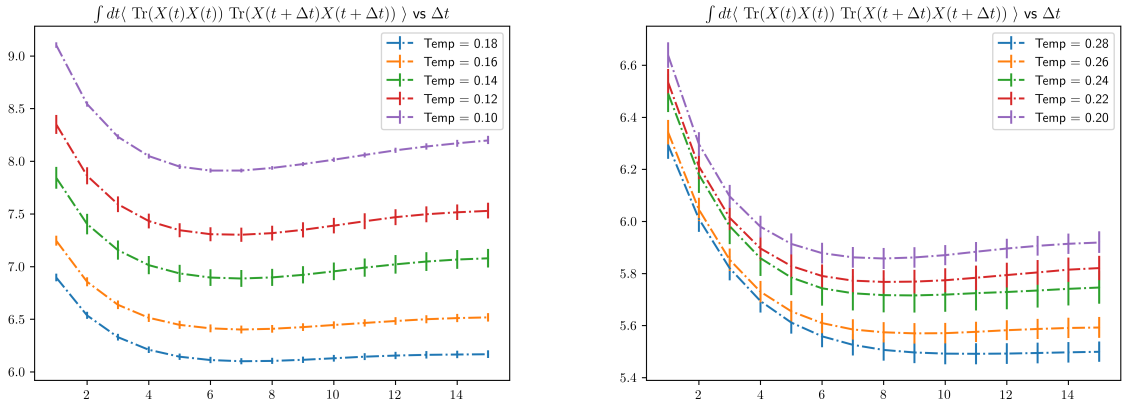

(a) Temperatures 0.10 - 0.18

(b) Temperatures 0.20 - 0.28

Figure 3: Gauge invariant 4-point correlators for different temperatures, obtained from the C++ code, with Number of colors = 9 and Number of lattice sites = 32

It is important to note that the correlator exhibits symmetry about $\Delta t =$ (Number of lattice sites)/2 due to the periodic boundary conditions imposed. Consequently, we have truncated the graphical representation to $\Delta t = 16$. Furthermore, it should be noted that the correlator lacks a normalization factor and an overall term that should be subtracted from it. The graphs presented here, as well as those that follow, are intended solely to illustrate the behavior of the correlator.

The expected behavior of the correlator is that of an exponential decay, from which one can extract the mass gap of the theory. In our studies, upon examination, it is evident that as the temperature decreases, the correlator's behavior deviates from the anticipated exponential decay and displays some oscillatory behavior.

To verify that this behavior is not due to an error in the relatively new C++ implementation, we implemented the correlator observable in the existing and stringently tested FORTRAN codebase of the MCSMC collaboration and performed the simulation for the same set of parameters as in the C++ code.

Subsequently, we conducted a comparative analysis of the results after going through the statistical analysis, the results which are as follows

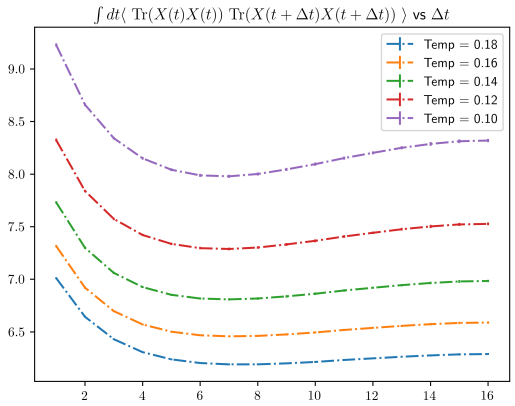

(a) Temperatures 0.10 - 0.18

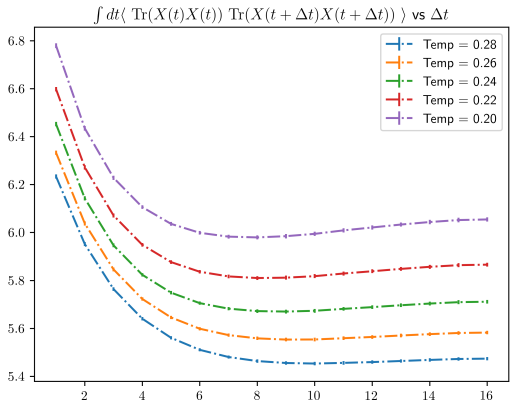

(b) Temperatures 0.20 - 0.28

Figure 4: Gauge invariant 4-point correlators for different temperatures, obtained from the FORTRAN code, with Number of colors = 9 and Number of lattice sites = 32

The results from the FORTRAN code exhibit the same behavior as those from the C++ code. To pinpoint the source of the anomalous behavior, we also considered a few other cases of the correlators, which are presented below.

Correlators for 3 and 6 colors

We computed the correlators for $N = 3$ and $N = 6$ with a lattice size 16, for a fixed temperature $T = 0.1$ to scrutinize the source of the anomalous behavior. The results are as follows:

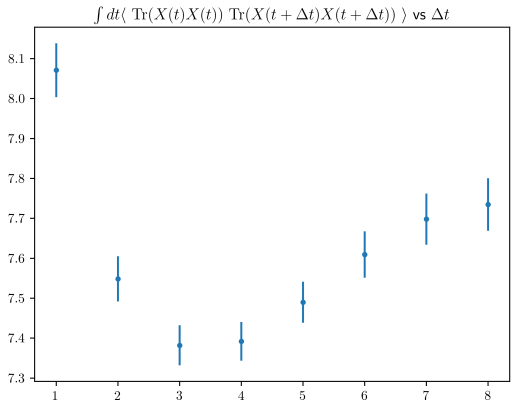

(a) Simulation for $N = 3$

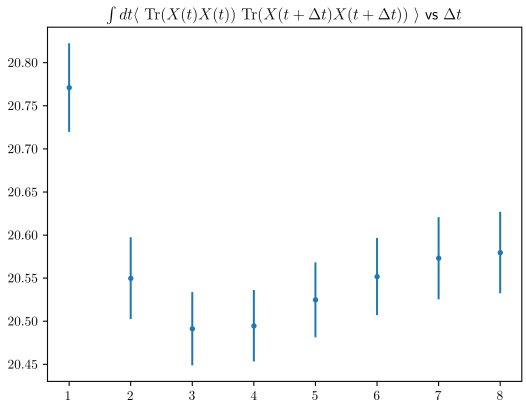

(b) Simulation for $N = 6$

Figure 5: Correlators for smaller values of N, with Temperature = 0.1 and 16 lattice sites

We observe that the oscillatory behavior persists even for smaller colors.

Single Matrix Correlators-Type Observables

We also consider two other observables

- $\int dt \langle \mathrm{Tr}(X^0(t)X^0(t))\ \mathrm{Tr}(X^0(t+\Delta t)X^0(t+\Delta t))\rangle$
- $\int dt \langle \mathrm{Tr}(X^0(t)X^1(t))\ \mathrm{Tr}(X^0(t+\Delta t)X^1(t+\Delta t))\rangle$

with $N = 9$, 16 lattice sites and Temperature 0.1. The results of the simulations are as follows:

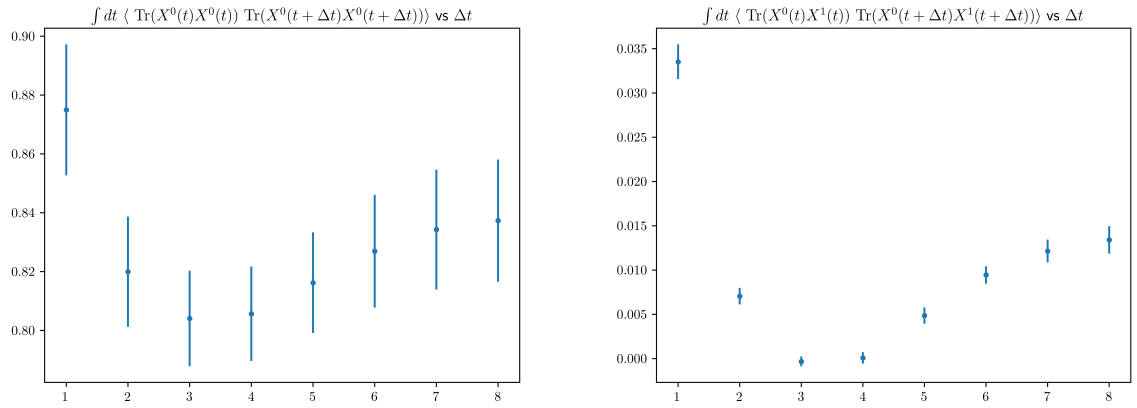

(a) Simulation for single matrix observable

(b) Simulation for single (mixed) matrix observable

Figure 6: Single matrix correlators, with Number of colors = 9, Number of lattice sites = 32 and Temperature = 0.1

We see that even in single matrix cases, and in mixed cases too, the correlator exhibits some oscillatory behavior. This behavior, therefore, is a feature of the model itself and is not a numerical artifact arising from the simulation errors.

Correlators in Free Theory

To investigate the origin of this behavior, we also simulated the behavior for the case when there is no commutator term in the action, that is, the free theory case

$$S_M = \frac{1}{g^2}\int dt\, \mathrm{Tr}\left\{\frac{1}{2}(D_0 X_M)^2\right\} \tag{27}$$

In this case, the correlator exhibits a decaying behavior as expected. The results of the simulation for Temperature=0.10, Number of colors = 9, Number of lattice sites = 16 is as follows:

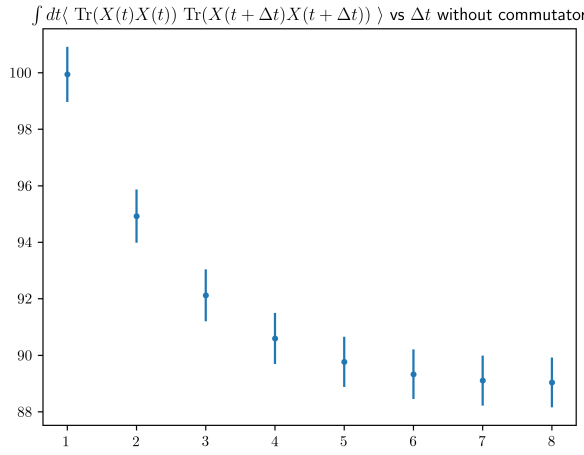

Figure 7: Complete 4-point gauge invariant correlator in free theory, with Temperature = 0.10, Number of colors = 9 and Number of lattice sites = 16

Correlators in the complete model with Fermions

FInally, we investigated the behavior of the correlator under the complete action of the BFSS model. For this, we employ the FORTRAN implementation of the code. This choice is motivated by the superior computational efficiency of the FORTRAN code as compared to the C++ code which is currently under development, particularly for Fermionic simulations, which are significantly more resource-intensive compared to their Bosonic counterparts. The results are as follows:

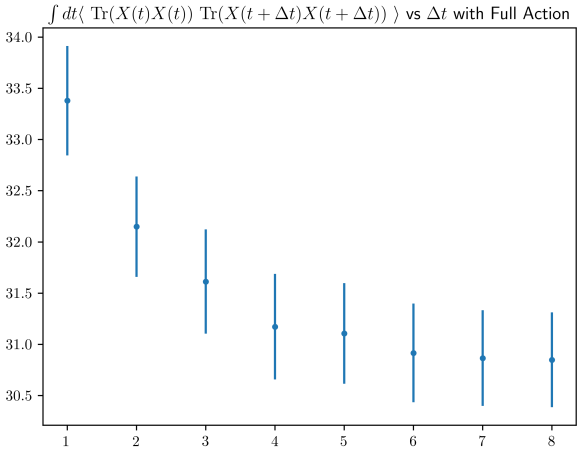

Figure 8: 4-point gauge invariant correlator in theory with the full action including the Fermionic sector. Temperature = 0.10, Number of colors = 3 and Number of lattice sites = 16

The correlators in the complete theory with fermions exhibit a decaying behavior as expected.

6 Conclusions

We have successfully implemented the lattice simulation for the BFSS model, both the Bosonic and Fermionic sectors, along with the required statistical methods for the analysis. We have also studied the behavior of the correlators in the Bosonic sector. We have shown that the correlators exhibit some oscillatory behavior and that this behavior is a feature of the model itself and is not a numerical artifact arising from the simulation errors.

Further analysis revealed that when the commutator (interaction) term in the action is turned off, the correlator reverts to the expected exponential decay behavior. This leads us to conclude that within the purely Bosonic sector, the presence of the $X - X$ interaction term is responsible for the observed anomalous behavior.

Interestingly, when considering the complete action inclusive of the Fermionic terms, the correlator demonstrates the expected exponential decay. However, the underlying mechanism by which the Fermionic terms suppress the anomalous behavior remains unclear and requires further investigation.

Some similar studies indicate that such an oscillatory behavior is a sign of the model exhibiting confinement [2, 3]. This translates to the statement that the glueballs in the Bosonic sector of the BFSS model are confined. However, such a statement here would require further theoretical and numerical verification to be stated concretely and can be only stated now as a speculation and not a conclusive statement.

References

[1] C. Gattringer and C. B. Lang, *Quantum Chromodynamics on the Lattice: An Introductory Presentation*, vol. 788 of *Lecture Notes in Physics*. Berlin, Heidelberg: Springer Berlin Heidelberg, 2010.

[2] O. Oliveira, D. Dudal, and P. J. Silva, "Glueball spectral densities from the lattice," Oct. 2012. arXiv:1210.7794 [hep-lat, physics:hep-ph, physics:hep-th].

[3] L. C. Loveridge, O. Oliveira, and P. J. Silva, "Schwinger function, confinement, and positivity violation in pure gauge QED," *Physical Review D*, vol. 106, p. L011502, July 2022.

[4] V. G. Filev and D. O'Connor, "The BFSS model on the lattice," *Journal of High Energy Physics*, vol. 2016, p. 167, May 2016. arXiv:1506.01366 [hep-lat, physics:hep-th].

[5] M. Hanada, J. Nishimura, Y. Sekino, and T. Yoneya, "Direct test of the gauge-gravity correspondence for Matrix theory correlation functions," *Journal of High Energy Physics*, vol. 2011, p. 20, Dec. 2011. arXiv:1108.5153 [hep-lat, physics:hep-th].

[6] E. Berkowitz, E. Rinaldi, M. Hanada, G. Ishiki, S. Shimasaki, and P. Vranas, "Precision lattice test of the gauge/gravity duality at large-N," *Physical Review D*, vol. 94, p. 094501, Nov. 2016. arXiv:1606.04951 [hep-lat, physics:hep-th].

[7] Y. Asano, V. G. Filev, S. Kováčik, and D. O'Connor, "The non-perturbative phase diagram of the BMN matrix model," *Journal of High Energy Physics*, vol. 2018, p. 152, July 2018. arXiv:1805.05314 [hep-th].

[8] M. Hanada, "What lattice theorists can do for superstring/M-theory," *International Journal of Modern Physics A*, vol. 31, p. 1643006, Aug. 2016. arXiv:1604.05421 [hep-lat, physics:hep-ph, physics:hep-th].

[9] T. Anous and C. Cogburn, "Mini-BFSS matrix model in silico," *Physical Review D*, vol. 100, p. 066023, Sept. 2019. Publisher: American Physical Society.

[10] A. Bilal, "M(atrix) Theory : a Pedagogical Introduction," *Fortschritte der Physik*, vol. 47, pp. 5–28, Jan. 1999. arXiv:hep-th/9710136.

[11] G. Bergner, N. Bodendorfer, M. Hanada, E. Rinaldi, A. Schafer, and P. Vranas, "Thermal phase transition in Yang-Mills matrix model," *Journal of High Energy Physics*, vol. 2020, p. 53, Jan. 2020. arXiv:1909.04592 [hep-lat, physics:hep-th].

[12] S. Pateloudis, G. Bergner, M. Hanada, E. Rinaldi, A. Schäfer, P. Vranas, H. Watanabe, and N. Bodendorfer, "Precision test of gauge/gravity duality in D0-brane matrix model at low temperature," *Journal of High Energy Physics*, vol. 2023, p. 71, Mar. 2023. arXiv:2210.04881 [hep-lat, physics:hep-th].

[13] B. Ydri, "Review of M(atrix)-Theory, Type IIB Matrix Model and Matrix String Theory," Nov. 2018. arXiv:1708.00734 [hep-lat, physics:hep-th].

[14] N. Kawahara, J. Nishimura, and S. Takeuchi, "High temperature expansion in supersymmetric matrix quantum mechanics," *Journal of High Energy Physics*, vol. 2007, pp. 103–103, Dec. 2007. arXiv:0710.2188 [hep-lat, physics:hep-th].

[15] M. Hanada, "BFSS code manual."

[16] R. Jackiw, "Introduction to the Yang-Mills quantum theory," *Reviews of Modern Physics*, vol. 52, pp. 661–673, Oct. 1980. Publisher: American Physical Society.

[17] A. Balachandran, V. Nair, and S. Vaidya, "Aspects of boundary conditions for non-Abelian gauge theories," *Physical Review D*, vol. 100, p. 045001, Aug. 2019. Publisher: American Physical Society.

[18] M. Daniel and C. M. Viallet, "The geometrical setting of gauge theories of the Yang-Mills type," *Reviews of Modern Physics*, vol. 52, pp. 175–197, Jan. 1980. Publisher: American Physical Society.